Global Biogeochemical Cycles

RESEARCH ARTICLE
10.1029/2021GB006949

Key Points:

- pH is controlled by the balance of thermal components via acid-base equilibrium and nonthermal components mainly via CO_2 addition/removal
- Carbonate saturation state (Ω) is dominated by nonthermal components mainly via external CO_2 addition/removal
- These differences explain why surface pH and Ω are often out of phase in spatial patterns and seasonal cycles

Supporting Information:

Supporting Information may be found in the online version of this article.

Correspondence to:

L. Xue,
xueliang@fio.org.cn

Citation:

Xue, L., Cai, W.-J., Jiang, L.-Q., & Wei, Q. (2021). Why are surface ocean pH and $CaCO_3$ saturation state often out of phase in spatial patterns and seasonal cycles? *Global Biogeochemical Cycles*, *35*, e2021GB006949. https://doi.org/10.1029/2021GB006949

Received 22 JAN 2021
Accepted 10 JUN 2021

Why are Surface Ocean pH and $CaCO_3$ Saturation State Often out of Phase in Spatial Patterns and Seasonal Cycles?

Liang Xue[1,2,3], Wei-Jun Cai[4], Li-Qing Jiang[5,6], and Qinsheng Wei[1]

[1]First Institute of Oceanography, and Key Laboratory of Marine Science and Numerical Modeling, Ministry of Natural Resources, Qingdao, China, [2]Laboratory for Regional Oceanography and Numerical Modeling, Qingdao National Laboratory for Marine Science and Technology, Qingdao, China, [3]Shandong Key Laboratory of Marine Science and Numerical Modeling, Qingdao, China, [4]School of Marine Science and Policy, University of Delaware, Newark, DE, USA, [5]Earth System Science Interdisciplinary Center, University of Maryland, College Park, MD, USA, [6]National Centers for Environmental Information, National Oceanic and Atmospheric Administration, Silver Spring, MD, USA

Abstract As two most important metrics for ocean acidification (OA), both pH and calcium carbonate mineral saturation states (Ω) respond sensitively to anthropogenic carbon dioxide (CO_2). However, contrary to intuition, they are often out of phase in the global surface ocean, both spatially and seasonally. For example, during warm seasons, Ω is lowest at high-latitude seas where there are very high pH values, challenging our understanding that high-latitude seas are a bellwether for global OA. To explain this phenomenon, we separate spatial and seasonal variations of both pH and Ω into thermal components mainly associated with internal acid-base equilibrium of seawater CO_2 systems, and nonthermal components mainly associated with external CO_2 addition/removal using a global surface ocean climatological data set. We find that surface pH change is controlled by the balance between its thermal and nonthermal components, which are out of phase but comparable in magnitude. In contrast, surface Ω change is dominated by its nonthermal components, with its thermal components in phase and significantly smaller in magnitude. These findings explain why surface ocean pH and Ω are often out of phase in spatial patterns and seasonal cycles. When pH is primarily controlled by nonthermal components e.g., gas exchange, mixing and biology, pH and Ω will be in phase because their nonthermal components are intrinsically in phase. In comparison, when pH is primarily controlled by thermal components for example, rapid seasonal cooling or warming, pH and Ω will be out of phase because thermal and nonthermal components of pH are out-of-phase in nature.

Plain Language Summary Although both pH and calcium carbonate mineral saturation states (Ω) are good metrics for ocean acidification, in the global surface ocean their spatial patterns and seasonal cycles are often out of phase, which appears counter intuitive. To explain this, we separate pH and Ω changes into thermal and nonthermal components. Thermal components are mainly related to the temperature driven internal acid-base equilibrium of seawater CO2 systems. Nonthermal components are the remaining changes, reflecting the effects of other non-temperature processes such as air-sea gas exchange, mixing and biology or a combination of these processes. We find that pH is controlled by the balance between thermal and nonthermal components, which are out of phase but comparable in magnitude, while Ω is almost always dominated by nonthermal components. These findings explain why surface ocean pH and Ω are often out of phase in spatial patterns and seasonal cycles. When pH is more controlled by nonthermal components than thermal components, pH and Ω will be in phase since their nonthermal components are intrinsically in phase. In contrast, when pH is more controlled by thermal components, pH and Ω will be out of phase because of the out-of-phase between thermal and nonthermal components of pH.

1. Introduction

Since the beginning of the Industrial Revolution, the global ocean has been taking up over two trillion tons of anthropogenic carbon dioxide (CO_2), which increases seawater hydrogen ion concentrations ($[H^+]$), and thus decreases pH, carbonate ion concentrations ($[CO_3^{2-}]$) and calcium carbonate mineral saturation states

(Ω), a process commonly known as ocean acidification (OA) (Caldeira & Wickett, 2003; Doney et al., 2009; Gruber, Clement et al., 2019). OA is usually characterized by decreases of pH or Ω over decades or longer timescales (Cooley et al., 2012; Jiang et al., 2015; Jiang et al., 2019). In the past decades declines in both pH and Ω have been observed through mooring stations and repeated hydrography lines (e.g., Dore et al., 2009; Takahashi et al., 2014; Lauvset et al., 2015). OA may have substantial negative influences on marine organisms and biogeochemical cycles (e.g., Cai, Feely et al., 2020; Doney et al., 2020; Wang et al., 2020), and thus receives ever increasing attention.

However, in the global surface ocean pH and Ω are often out of phase in terms of spatial patterns and seasonal cycles, which appears counter intuitive (Kwiatkowski & Orr, 2018; Takahashi et al., 2014), though both of them have been widely used as good metrics for OA. For example, during February, the Southern Ocean Ω is almost the lowest among all ocean basins while its pH values are very high (Takahashi et al., 2014). Therefore, from the already very low Ω point of view, surface waters of the high latitudes are most vulnerable to anthropogenic-induced acidification and serve as a bellwether for global OA (Fabry et al., 2009). However, from the high pH point of view, these waters are not necessarily the most vulnerable in the global ocean. Similar examples can be found in the northern subarctic waters (Cai, Xu et al., 2020). This challenges our understanding that high-latitude seas are a bellwether for global OA. Seasonally, for instance at 25°N sea surface pH and Ω are out of phase, with pH showing the maximum in February-March and the minimum in August-September, and Ω showing the minimum in February-March and the maximum in August-September (Kwiatkowski & Orr, 2018). In contrast, at 50°N sea surface pH and Ω are almost in phase, with the minimum in January-February and the maximum in June-July (Kwiatkowski & Orr, 2018). Furthermore, the out-of-phase nature between pH and Ω variations would further complicate the debate as to whether pH or Ω is a better indicator of the influences of carbonate chemistry on marine organisms (Jokiel, 2013; Riebesell, 2004; Waldbusser et al., 2014), since biological influences depend on the superimposition of long-term changes and short-term natural variabilities (Kwiatkowski & Orr, 2018; Landschützer et al., 2018; McNeil & Matear, 2008; Mcneil & Sasse, 2016). Thus, it is of uttermost importance to clarify why surface ocean pH and Ω are often out of phase in spatial patterns and seasonal cycles, particularly with increasing interests in OA in the future.

2. Thermal and Nonthermal Components of Ocean pH and Ω

Thermal components are related to the temperature driven internal acid-base equilibrium of seawater CO_2 systems. They mainly refer to changes in pH, Ω and CO_2 partial pressure (pCO_2) due to temperature effects on the CO_2 solubility constant (K_0), the apparent dissociation constants of carbonic acid (K_1 and K_2) and the apparent solubility product (K_{sp}) of calcium carbonate ($CaCO_3$) in a closed system with no gas exchange with the atmosphere. They are calculated under conditions of constant total alkalinity (TA), total dissolved inorganic carbon (DIC) and salinity (e.g., Cai, Xu et al., 2020; Jiang et al., 2019; Xue et al., 2020). For example, the pH correction made from measurement temperature to in situ temperature is special for adjusting the influence from thermal components (Gieskes, 1969). The same practice applies to the well-known pCO_2 normalization to a common temperature, which is carried out under a condition of constant TA, DIC and salinity (Takahashi et al., 2002). Nonthermal components are the remaining changes or total changes minus thermal components mainly via external CO_2 addition/removal, reflecting the effects of the remaining processes that can alter DIC and/or TA such as through air-sea exchange, mixing and biology or a combination of these processes (e.g., Gruber, Landschutzer et al., 2019). In terms of timescales, thermal components are almost instantaneous, while nonthermal components are not, depending on the timescale of the dominant process. Note that the separation of thermal and nonthermal components does not imply that the nonthermal components are not temperature sensitive. Rather, for example, the air-sea CO_2 flux is very much driven by the temperature dependent solubility constant particularly in oceans with shallow mixed layer depths (e.g., Xu et al., 2020; Xue et al., 2020).

By definition, the thermal components of pH and Ω are out of phase or have opposite signs. When temperature increases, in a closed system the dissociation of bicarbonate (HCO_3^-) (Equation 1) and water (H_2O) are the primary processes producing H^+. Despite the fact that most of the excess H^+ produced in this process will be consumed by reacting with borate ($B(OH)_4^-$) and HCO_3^-, the remaining new H^+ is enough to decrease pH noticeably (Cai, Xu et al., 2020; Jiang et al., 2019). On the other hand, the extra CO_3^{2-} from the

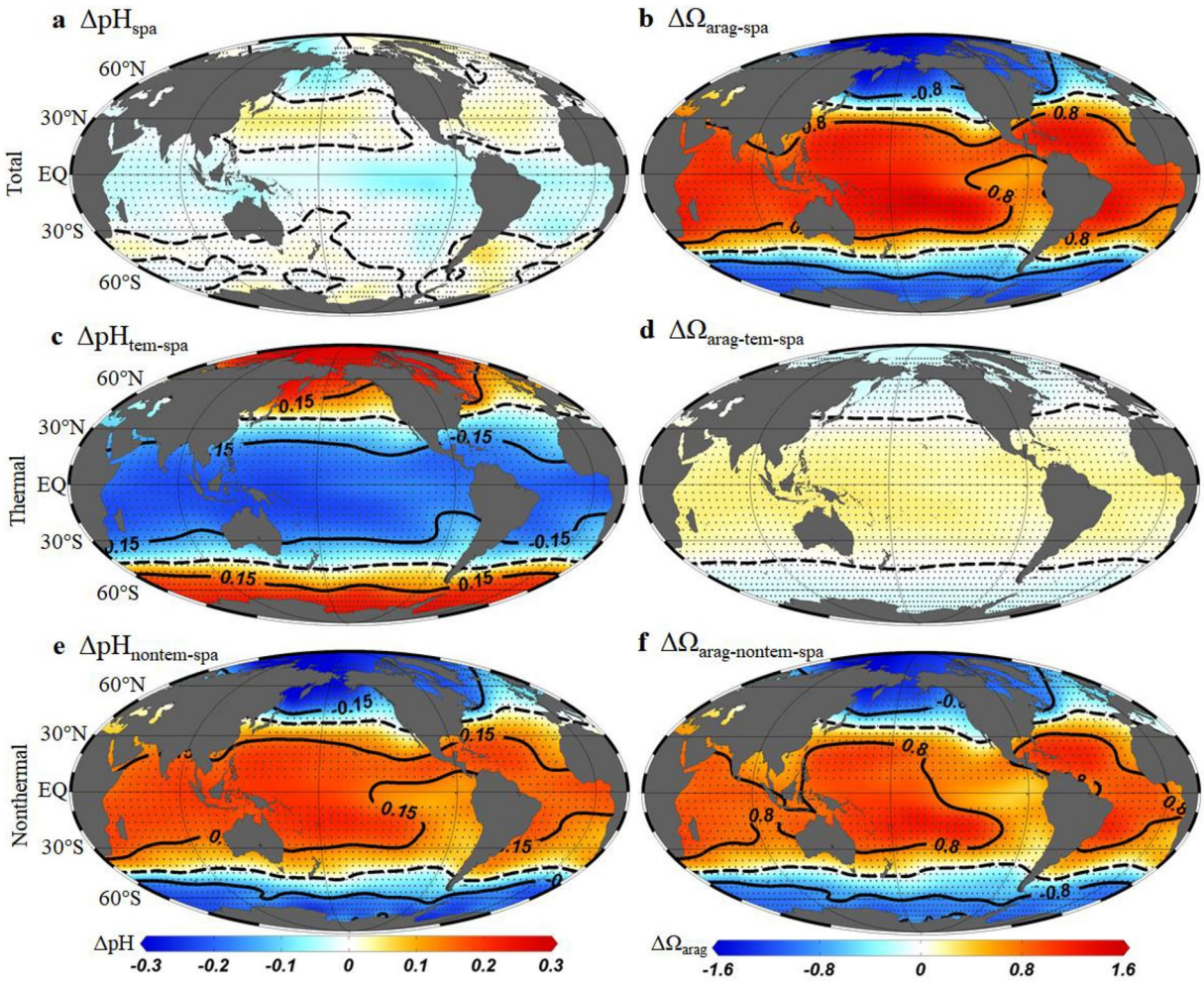

Figure 1. Relative spatial variability of climatological sea surface pH and Ω_{arag} during February (ΔpH_{spa} and $\Delta\Omega_{ara\text{-}spa}$, a–b) as well as their thermal ($\Delta pH_{tem\text{-}spa}$ and $\Delta\Omega_{arag\text{-}tem\text{-}spa}$, c–d) and nonthermal components ($\Delta pH_{nontem\text{-}spa}$ and $\Delta\Omega_{arag\text{-}nontem\text{-}spa}$, e-f). ΔpH_{spa} and $\Delta\Omega_{ara\text{-}spa}$ are the values relative to global mean values. Note as shown by the dots, climatological pH and Ω_{arag} data are not available in the equatorial zone (4°N–4°S) of the Pacific due to large interannual variabilities associated with ENSO events (Takahashi et al., 2014) (also hereafter). Black lines denote isolines and the dashed ones show those with values of zero. Figures 1–4 and 6 are plotted using Ocean Data View (odv_4.7.10_w64 version) (Schlitzer, 2018).

dissociation of HCO_3^- (Equation 1), combined with a decrease of K_{sp} with temperature (Mucci, 1983) helps enhance Ω. Similarly, in a closed system cooling will increase pH but decrease Ω.

$$HCO_3^- \rightleftarrows H^+ + CO_3^{2-} \quad (1)$$

In contrast, the nonthermal components of pH and Ω, that is, those after removing thermal components, are in phase or have the same sign, since they both mainly reflect the relative change between TA and DIC such as their differences ([TA-DIC]) as discussed by Xue & Cai (2020). In short, by definition (TA-DIC = $CO_3^{2-} - CO_2^* +$ Borate alkalinity, here CO_2^* denotes the sum of true carbonic acid and aqueous carbon dioxide), [TA-DIC] as a combined property directly reflects influences from external CO_2 addition/removal, or the relative change of [CO_3^{2-}] and [CO_2^*] (pH) and the variability of [CO_3^{2-}] in normal seawaters (see their Figures 1 and 2). Consequently, [TA-DIC] shows very good positive relationships with temperature normalized pH and Ω, that is, their nonthermal components. For instance, adding CO_2 to seawater, which decreases [TA-DIC], will increase [H^+] but decrease [CO_3^{2-}], resulting in declines both in pH and Ω (e.g., Doney et al., 2009). Thus, given the in-phase nature between the nonthermal components of pH and Ω, the out-of-phase between pH and Ω in spatial patterns and seasonal cycle must originate from the difference in their thermal components.

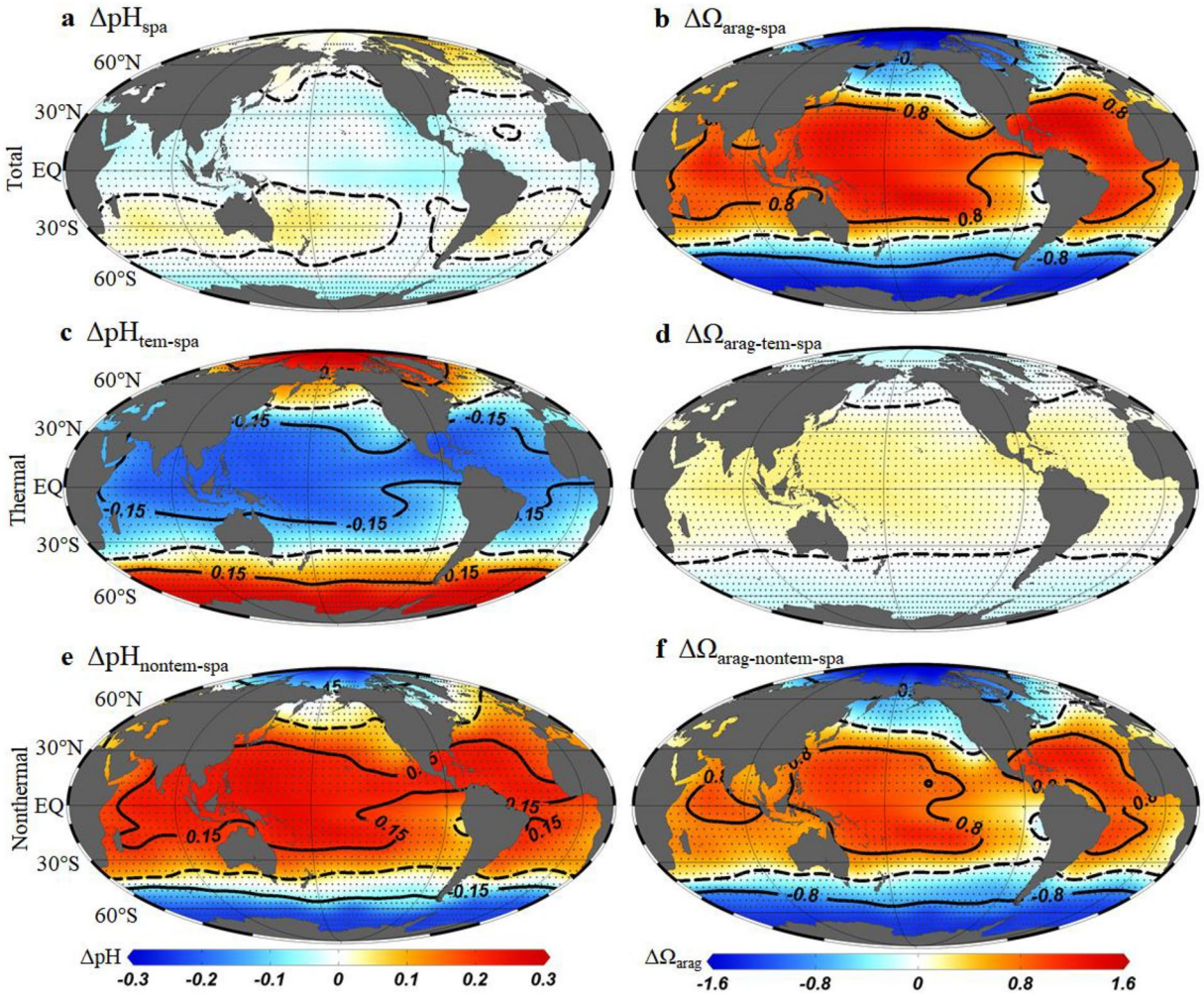

Figure 2. Relative spatial variability of climatological sea surface pH and Ω_{arag} during August (ΔpH_{spa} and $\Delta\Omega_{ara\text{-}spa}$, a–b) as well as their thermal ($\Delta pH_{tem\text{-}spa}$ and $\Delta\Omega_{arag\text{-}tem\text{-}spa}$, c–d) and nonthermal components ($\Delta pH_{nontem\text{-}spa}$ and $\Delta\Omega_{arag\text{-}nontem\text{-}spa}$, e–f). ΔpH_{spa} and $\Delta\Omega_{ara\text{-}spa}$ are the values relative to global mean values. Black lines denote isolines and the dashed ones show those with values of zero.

2.1. Hypothesis for pH and Ω

In a hypothetical ocean system that allows temperature change and rapid temperature driven air-sea CO_2 equilibrium, the thermal and nonthermal components of pH are out of phase, but for Ω they are in phase. For instance, when sea surface temperature (SST) increases, the thermal components, which does not allow gas exchange, will lower pH but elevate Ω (Equation 1). While the nonthermal components, which here are solely due to the temperature induced air-sea CO_2 exchange, will enhance both pH and Ω, since increasing temperature will increase seawater pCO_2, allowing a body of water to release more CO_2 in order to maintain equilibrium with the atmosphere. By using the CO_2SYS tools (Lewis & Wallace, 1998), Jiang et al. (2019) and Xue et al. (2020) show that in this simplified ocean system the thermal and nonthermal components of pH are comparable in magnitude, while Ω is dominated by nonthermal components. For example, if we could move a body of water from the polar area (~0°C) to the tropical area (~30°C), the thermal and nonthermal components would make pH change by −0.47 and 0.46 units, respectively, thus nearly fully canceled each other. In contrast, during this process the thermal and nonthermal components would make Ω increase by ~15% and ~50%, respectively (Jiang et al., 2019). Therefore, in this rapid gas exchange case, the thermal and nonthermal components almost have an equally important influence on pH with similar magnitudes but tend to cancel each other whereas they have an additive influence on Ω (also see Figures 1e and 1f in Cai, Xu et al., (2020)).

In this context, we propose a hypothesis that in real ocean conditions which are often under air-sea disequilibrium and have complicated physical and biological processes, pH would be either more controlled by its thermal or nonthermal components, depending on their competing effects because these two components are out of phase but comparable in magnitude, while Ω would be almost always dominated by its nonthermal components. If this hypothesis works, it would well explain why the global surface ocean pH and Ω are often out of phase in terms of spatial patterns and seasonal cycles. Given that Ω would be almost always dominated by its nonthermal components, when pH is more controlled by nonthermal components than thermal components, pH and Ω will be in phase since their nonthermal components are intrinsically in phase; when pH is more controlled by thermal components, pH and Ω will be out phase since the thermal and nonthermal components of pH are out of phase and the nonthermal components of pH and Ω are in phase. In this study, we examine this hypothesis in the global surface ocean by calculating the thermal and nonthermal components of pH and Ω with climatological data from the Lamont-Doherty Earth Observatory (LDEO) Takahashi Database (Takahashi et al., 2014).

2.2. Calculation of Thermal and Nonthermal Components of pH and Ω

Following the approach used by Landschützer et al. (2018) for pCO_2, we separate pH and Ω into thermal and nonthermal components. To calculate them, we first calculate the climatological monthly pH and Ω at a 4 × 5° grid over the global surface ocean with pCO_2 and TA data as well as temperature, salinity, phosphate, and silicate data from the LDEO Takahashi Database (https://www.nodc.noaa.gov/ocads/oceans/ndp_094/ndp094.html). Only seawater saturation state with respect to the mineral aragonite (Ω_{arag}) is calculated according to Equation 2, since both aragonite and calcite are common polymorphs of $CaCO_3$ in the ocean (Morse et al., 2007), aragonite is more soluble than calcite in an almost constant ratio of 1.5 (Mucci, 1983), and their spatial patterns and seasonal cycle are almost identical (Takahashi et al., 2014).

$$\Omega_{arag} = \left[CO_3^{2-}\right] \times \left[Ca^{2+}\right] / K_{K_{sp-arag}} \tag{2}$$

where $[Ca^{2+}]$ is the calcium concentration and $K_{sp\text{-}arag}$ is the apparent solubility product of aragonite (Mucci, 1983). Sea surface $[Ca^{2+}]$ is calculated from salinity (0.010260/35 × salinity mol kg^{-1}) based on the conservative behavior of $[Ca^{2+}]$ to salinity (Riley & Tongudai, 1967), and $K_{sp\text{-}arag}$ is calculated after Mucci (1983).

Given the fact that in surface waters of the open ocean $[Ca^{2+}]$ is conservative with respect to salinity, both pH and Ω_{arag} can be expressed as a function of TA, DIC, salinities (S) and temperatures (T) (e.g., Xue et al., 2016), that is, f(TA, DIC, S, T). Below we take pH as an example and show the calculation of its thermal and nonthermal components (similar calculation is done for Ω_{arag}) using the LDEO Takahashi Database. All these calculations are done with the MATLAB version of the CO_2SYS program (Lewis & Wallace, 1998; van Heuven et al., 2009), using the apparent dissociation constants for carbonic acid of Mehrbach et al. (1973) as refitted by Dickson and Millero (1987) and the CO_2 solubility constant of Weiss (1974).

2.2.1. Spatial Patterns of Surface pH and its Thermal and Nonthermal Components

To clearly exhibit the spatial patterns of pH and Ω_{arag}, we calculate the relative spatial variability for pH and Ω_{arag} at the grid (ΔpH_{spa} and $\Delta\Omega_{arag\text{-}spa}$), that is, the values relative to global mean values. Calculations of ΔpH_{spa} as well as their thermal ($\Delta pH_{tem\text{-}spa}$) and nonthermal ($\Delta pH_{nontem\text{-}spa}$) components are shown in Equation 3. Also, relative spatial variability for SST and [TA-DIC] (ΔSST_{spa} and $\Delta[TA\text{-}DIC]_{spa}$) are calculated similarly as in Equation 3a.

$$\Delta pH_{spa} = pH_{grid} - pH_{mean} \tag{3a}$$

$$\Delta pH_{tem\text{-}spa} = f\left(TA_{mean}, DIC_{mean}, S_{mean}, T_{grid}\right) - f\left(TA_{mean}, DIC_{mean}, S_{mean}, T_{mean}\right) \tag{3b}$$

$$\Delta pH_{nontem\text{-}spa} = \Delta pH_{spa} - \Delta pH_{tem\text{-}spa} \tag{3c}$$

where pH_{grid} and T_{grid} are monthly mean values at grids, and TA_{mean}, DIC_{mean}, S_{mean} and T_{mean} are global mean values during the selected month (February and August).

In addition, relative importance (rpH_{spa}) of nonthermal and thermal components for ΔpH_{spa} is calculated as the ratio of their respective absolute values:

$$rpH_{spa} = \left|\Delta pH_{nontem\text{-}spa}\right| / \left|\Delta pH_{tem\text{-}spa}\right| \quad (3d)$$

A rpH_{spa} value of <1 indicates a stronger control of thermal components over ΔpH_{spa} than nonthermal components, while a rpH_{spa} value of >1 indicates a stronger control of nonthermal components. Similar calculations are done for thermal and nonthermal components of $\Delta\Omega_{arag\text{-}spa}$, that is, $\Delta\Omega_{arag\text{-}tem\text{-}spa}$ and $\Omega_{arag\text{-}nontem\text{-}spa}$ as well as for their relative importance, that is, $r\Omega_{arag\text{-}spa}$.

2.2.2. Seasonal Cycles of Surface pH and its Thermal and Nonthermal Components

To examine the difference between pH and Ω in phases of seasonal cycles, we calculate thermal and nonthermal pH or Ω which is just controlled by thermal components or nonthermal components in each month at some typical grids covering different latitudinal belts (Figure S1), that is, pH_{tem}, pH_{nontem}, $\Omega_{arag\text{-}tem}$ and $\Omega_{arag\text{-}nontem}$. Specifically, pH_{tem} in each month ($pH_{tem(t)}$) is calculated using constant TA, DIC and S, which here are values in January (TA_1, DIC_1 and S_1), and corresponding monthly mean temperature (T_t) at grids. pH_{nontem} in each month ($pH_{nontem(t)}$) is calculated using constant T, which here is value in January (T_1), and corresponding monthly mean TA, DIC and S (TA_t, DIC_t and S_t) at grids. Calculations of $pH_{tem(t)}$ and $pH_{nontem(t)}$ are shown in Equation 4. Similar calculations are done for $\Omega_{arag\text{-}tem}$ and $\Omega_{arag\text{-}nontem}$. Note here selecting the values in January rather than the annual mean as constant values makes each component start from the same point (January), clearly exhibiting the contributions of thermal and nonthermal components on in situ pH and Ω_{arag}.

$$pH_{tem(t)} = f\left(TA_1, DIC_1, S_1, T_t\right) \quad (4a)$$

$$pH_{nontem(t)} = f\left(TA_t, DIC_t, S_t, T_1\right) \quad (4b)$$

Further, following Takahashi et al. (2014), we calculate the seasonal amplitude of pH and Ω_{arag} (ΔpH_{sea} and $\Delta\Omega_{arag\text{-}sea}$) between winter (period 1) and summer (period 2). The mean values of pH and Ω_{arag} during these two periods are calculated from the corresponding mean values of TA, DIC, S and T using the CO_2SYS program (Lewis & Wallace, 1998). Related parameters during the boreal winter period (January-February-March) are set as TA_{sea1}, DIC_{sea1}, S_{sea1} and T_{sea1}, respectively, and those during the boreal summer period (July-August-September) are set as TA_{sea2}, DIC_{sea2}, S_{sea2} and T_{sea2}, respectively. Calculations of ΔpH_{sea} as well as their thermal ($\Delta pH_{tem\text{-}sea}$) and nonthermal ($\Delta pH_{nontem\text{-}sea}$) components are shown in Equation 5. Also, the seasonal amplitude of SST and [TA-DIC] (ΔSST_{sea} and $\Delta[TA\text{-}DIC]_{sea}$) are calculated similarly as in Equation 5a.

$$\Delta pH_{sea} = f\left(TA_{sea2}, DIC_{sea2}, S_{sea2}, T_{sea2}\right) - f\left(TA_{sea1}, DIC_{sea1}, S_{sea1}, T_{sea1}\right) \quad (5a)$$

$$\Delta pH_{tem\text{-}sea} = f\left(TA_{sea2}, DIC_{sea2}, S_{sea2}, T_{sea2}\right) - f\left(TA_{sea2}, DIC_{sea2}, S_{sea2}, T_{sea1}\right) \quad (5b)$$

$$\Delta pH_{nontem\text{-}sea} = \Delta pH_{sea} - \Delta pH_{tem\text{-}sea} \quad (5c)$$

Similar calculations are done for thermal and nonthermal components of $\Delta\Omega_{arag\text{-}sea}$, that is, $\Delta\Omega_{arag\text{-}tem\text{-}sea}$ and $\Omega_{arag\text{-}nontem\text{-}sea}$. Also, the relative importance of nonthermal and thermal components for both ΔpH_{sea} and $\Delta\Omega_{arag\text{-}sea}$, that is, rpH_{sea} and $r\Omega_{arag\text{-}sea}$ is calculated similarly as in Equation 3d. Value of <1 indicates a stronger control of thermal components than nonthermal components, while value of >1 indicates a stronger control of nonthermal components.

3. Results and Discussion

3.1. Spatial Distributions of Sea Surface pH and Ω_{arag}

As the spatial patterns of surface pH and Ω_{arag} change with time, to fully appreciate them, we show their distributions in two representative months, that is, February (Figures 1a and 1b) and August (Figures 2a and 2b). We find that there are substantial differences between pH and Ω_{arag} in their spatial patterns (Figures 1 and 2). First, across the global surface ocean, it is conspicuous that Ω_{arag} values in the high-latitudes of both hemispheres are the lowest spatially with the relative spatial variability of Ω_{arag} or $\Delta\Omega_{arag\text{-}spa} < 0$ (Figures 1b and 2b), while pH values there are not always low (Figures 1a and 2a). During cold seasons of both hemispheres, similar to Ω_{arag}, pH has low values in high-latitudes. For example, in February there are low pH values in subpolar and polar waters of the northern hemisphere with the relative spatial variability of pH or $\Delta pH_{spa} < 0$ (Figure 1a), and in August there are low pH values in subpolar and polar waters of the Southern Ocean with $\Delta pH_{spa} < 0$ (Figure 2a). In contrast, during warm seasons of both hemispheres in high-latitudes there are high pH values spatially. In February there are relatively high pH values with $\Delta pH_{spa} > 0$ in subpolar and polar waters of the Southern Ocean (Figure 1a), and in August there are relatively high pH values with $\Delta pH_{spa} > 0$ in subpolar and polar waters of the northern hemisphere (Figure 2a). Therefore, with respect to pH, the surface ocean at high latitudes is not always the bellwether for global OA, whereas with respect to Ω_{arag}, surface waters at high latitudes are always particularly vulnerable to anthropogenic-induced acidification (Fabry et al., 2009). Second, in most parts of surface tropical and subtropical waters (low latitude) ΔpH_{spa} is negative (Figures 1a and 2a) whereas $\Delta\Omega_{arag\text{-}spa}$ is positive (Figures 1b and 2b) in these two months. In other words, spatially these waters have relatively lower pH values and higher Ω_{arag} values than the respective global mean value in the same month. Thus, from this point of view, one may choose pH in the tropical waters and Ω_{arag} in the polar waters as a bellwether or a better indicator for OA.

3.1.1. Influence of Thermal and Nonthermal Components on pH Spatial Patterns

To explore the difference between pH and Ω_{arag} in spatial patterns, based on the method described in Section 2.2.1, by separating ΔpH_{spa} and $\Delta\Omega_{arag\text{-}spa}$ into thermal and nonthermal components we test the hypothesis we propose in Section 2.1. We find that our hypothesis works for the spatial distribution of pH and Ω_{arag}.

In the global surface ocean, the thermal and nonthermal components of pH spatial distribution, that is, $\Delta pH_{tem\text{-}spa}$ and $\Delta pH_{nontem\text{-}spa}$ always have opposite signs (Figures 1 and 2). Above ~36° latitudes both in February and August, the sign of $\Delta pH_{tem\text{-}spa}$ is positive whereas the sign of $\Delta pH_{nontem\text{-}spa}$ is negative; between ~36°S and ~36°N the sign of $\Delta pH_{tem\text{-}spa}$ is negative, whereas the sign of $\Delta pH_{nontem\text{-}spa}$ is positive. The opposite signs between $\Delta pH_{tem\text{-}spa}$ and $\Delta pH_{nontem\text{-}spa}$ are caused by their intrinsic definitions. As analyzed in Section 2, by definition pH thermal components decrease with temperature and always have a negative correlation with temperature (Gieskes, 1969), while pH nonthermal components mainly reflect the relative change between TA and DIC via CO_2 addition/removal and present a positive correlation with [TA-DIC] (Xue & Cai, 2020). This is verified by the spatial variability of surface pH. $\Delta pH_{tem\text{-}spa}$ is negatively correlated with the relative spatial variability of SST or ΔSST_{spa} (Figures S2a and S3a) and always presents opposite patterns to ΔSST_{spa} (Figures 1–3), whereas $\Delta pH_{nontem\text{-}spa}$ is positively correlated with the relative spatial variability of [TA-DIC] or $\Delta[TA\text{-}DIC]_{spa}$ (Figures S2b and S3b) and exhibits similar patterns to $\Delta[TA\text{-}DIC]_{spa}$ (Figures 1–3). Interestingly, we find both $\Delta[TA\text{-}DIC]_{spa}$ and $\Delta pH_{nontem\text{-}spa}$ are positively correlated with ΔSST_{spa} (Figures 1–3 and S2, S3). This not only directly explains the opposite signs between $\Delta pH_{tem\text{-}spa}$ and $\Delta pH_{nontem\text{-}spa}$, but also indicates that $\Delta pH_{nontem\text{-}spa}$ or $\Delta[TA\text{-}DIC]_{spa}$ is mainly controlled by SST associated processes such as air-sea exchange, vertical mixing and biological activity. This is because high SST has the potential to remove CO_2 from surface ocean by degassing CO_2 to the atmosphere, weakening vertical mixing and enhancing biological production while low SST has the potential to add surface CO_2 (e.g., Keppler et al., 2020; Wu et al., 2019).

Further, we find that the thermal and nonthermal components of pH are comparable in magnitude. During February in the global surface ocean $\Delta pH_{tem\text{-}spa}$ ranges from −0.23 to 0.26, while $\Delta pH_{nontem\text{-}spa}$ varies between −0.32 and 0.23 (Figures 1c and 1e); during August in the global surface ocean $\Delta pH_{tem\text{-}spa}$ ranges from −0.22 to 0.28, while $\Delta pH_{nontem\text{-}spa}$ varies between −0.36 and 0.21 (Figures 2c and 2e). As a result, the pH thermal and nonthermal components partially cancel each other and greatly decrease the spatial variability of pH, with ΔpH_{spa} ranging from −0.12 to 0.17 during February and August in the global surface ocean (Figures 1a and 2a).

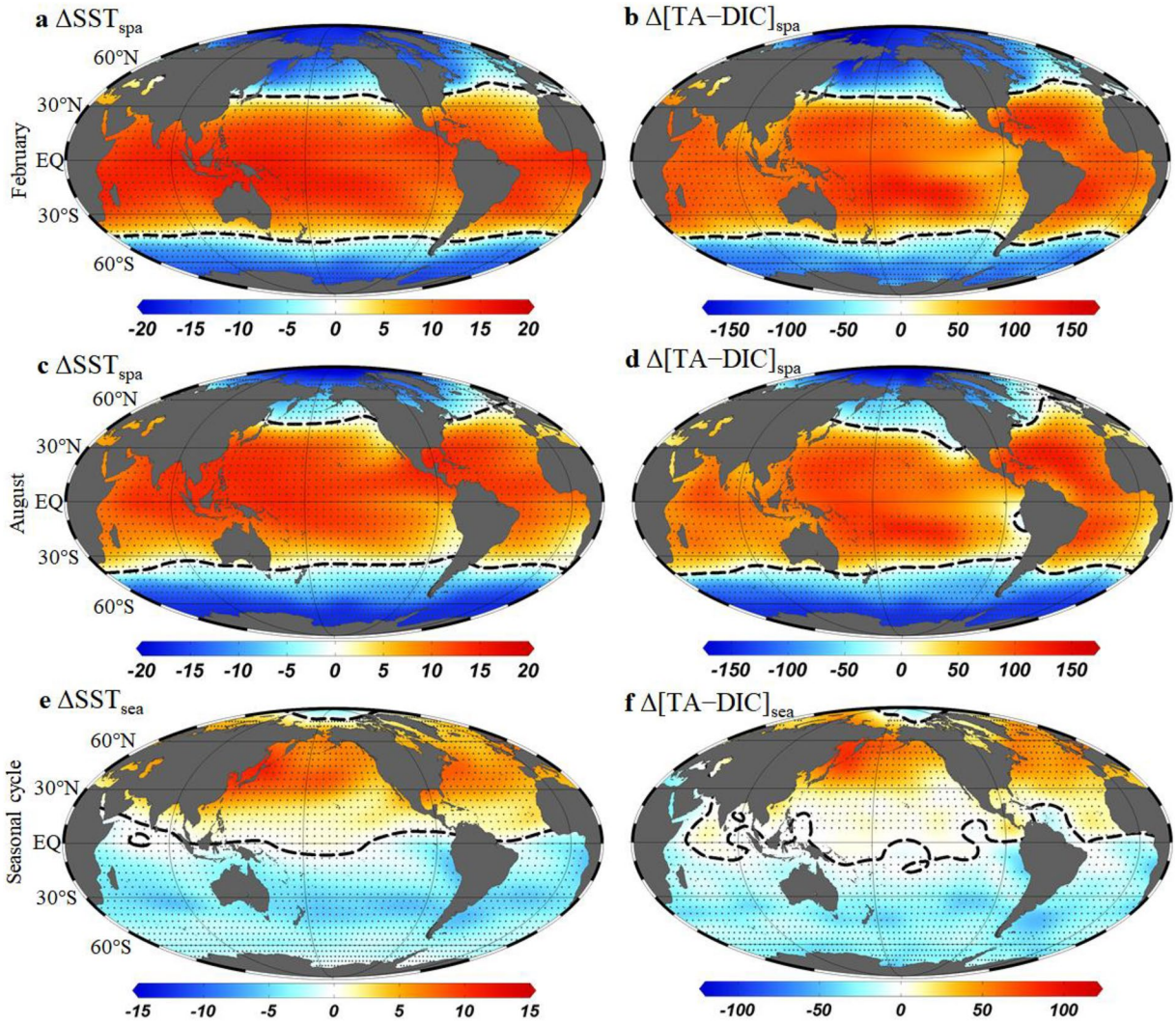

Figure 3. Relative spatial variability of climatological sea surface temperature and [TA-DIC] (ΔSST_{spa} and $\Delta[TA\text{-}DIC]_{spa}$) during February (a–b) and August (c–d), and their seasonal amplitude (ΔSST_{sea} and $\Delta[TA\text{-}DIC]_{sea}$, e-f). ΔSST_{spa} and $\Delta[TA\text{-}DIC]_{spa}$ are the values relative to global mean values, and the seasonal amplitude is given as the July-August-September mean value minus the January-February-March mean value as shown by Takahashi et al. (2014). Dashed lines denote isolines with values of zero. Units of ΔSST and Δ[TA-DIC] are °C and μmol kg^{-1}, respectively.

Consequently, the opposite signs but comparable magnitudes of pH thermal and nonthermal components determine that the spatial variability of pH is sometimes controlled more by thermal components than by nonthermal components and other times more by nonthermal components, depending on their net competing effects (Figures 4a and 4c). In mid-and-high latitudes, during cold seasons of both hemispheres the contribution from $\Delta pH_{tem\text{-}spa}$ is generally smaller than that from $\Delta pH_{nontem\text{-}spa}$ that is, the ratio between nonthermal components and thermal components (rpH_{spa}) > 1 (Figures 4a and 4c) and ΔpH_{spa} there is controlled more by nonthermal components than by thermal components; whereas during warm seasons rpH_{spa} there is generally less than 1 (Figures 4a and 4c) and ΔpH_{spa} is controlled more by thermal components than by nonthermal components. For example, in the Southern Ocean at 68°S, 172.5°W during August (cold season) when ΔSST_{spa} is −16.79°C, $\Delta pH_{tem\text{-}spa}$ is 0.27 and $\Delta pH_{nontem\text{-}spa}$ is −0.32, there is a net pH spatial change of −0.05, indicating a stronger control of nonthermal components on pH than thermal components; on the other hand, during February (warm season) when ΔSST_{spa} is −14.10°C, $\Delta pH_{tem\text{-}spa}$ is 0.23 and $\Delta pH_{nontem\text{-}spa}$ is −0.20, there is a net pH spatial change of 0.03, indicating a strong control of thermal components there. The alternative control of thermal and nonthermal components over pH spatial patterns in mid-and-high latitudes is mainly associated with the seasonality of biological activity and vertical mix-

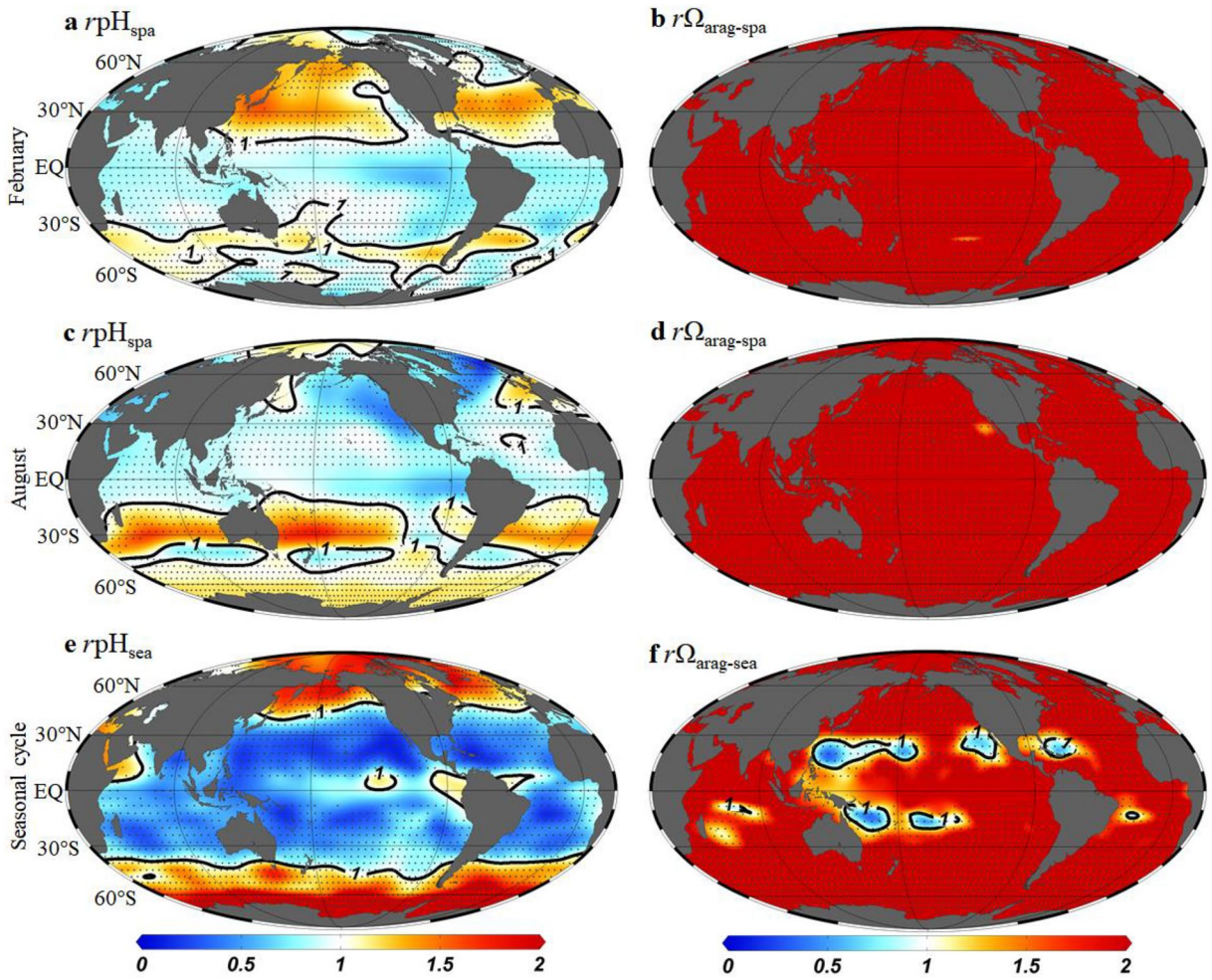

Figure 4. Ratios between nonthermal and thermal components for pH and Ω_{arag} relative spatial variability (rpH$_{spa}$ and $r\Omega_{arag\text{-}spa}$, a–d) and seasonal cycles (rpH$_{sea}$ and $r\Omega_{arag\text{-}sea}$, e-f). Panels (a) and (b) show the ratios during February, and panels (c) and (d) during August. Ratios of <1 (blue color) indicate a stronger control of thermal components on pH or Ω_{arag} than nonthermal components, while values of >1 (red color) indicate a stronger control of nonthermal components.

ing. For example, in the Southern Ocean there are stronger biological production and shallower mixed layer depth during February than during August (e.g., Gregor et al., 2018). Therefore, from August to February, these two processes would substantially reduce the magnitude of the nonthermal components (e.g., −0.32 vs.-0.20) and result in the switch from the primary control by nonthermal components during August (cold season) to the primary control by thermal components during February (warm season).

Different from mid-and-high latitudes, in most parts of surface tropical and subtropical waters (low latitude), regardless of seasons, the contribution from ΔpH$_{tem\text{-}spa}$ is generally larger than that from ΔpH$_{nontem\text{-}spa}$ that is, rpH$_{spa}$ < 1 (Figures 4a and 4c) and ΔpH$_{spa}$ there is controlled more by thermal components than by nonthermal components. For example, in the North Pacific at 12°N, 172.5°W (low-latitude), during February when ΔSST$_{spa}$ is 12.35°C, ΔpH$_{tem\text{-}spa}$ is −0.19 and ΔpH$_{nontem\text{-}spa}$ is 0.18, there is a net pH spatial change of −0.01, indicating a stronger control of thermal components on pH than nonthermal components; similarly during August when ΔSST$_{spa}$ is 13.50°C, ΔpH$_{tem\text{-}spa}$ is −0.20 and ΔpH$_{nontem\text{-}spa}$ is 0.18, there is a net pH spatial change of −0.02, also suggesting a stronger control of thermal components.

3.1.2. Influence of Thermal and Nonthermal Components on Ω_{arag} Spatial Patterns

Different from pH, in the global surface ocean the thermal and nonthermal components of Ω_{arag} spatial variability, that is, $\Delta\Omega_{arag\text{-}tem\text{-}spa}$ and $\Delta\Omega_{arag\text{-}nontem\text{-}spa}$ always present the same sign (Figures 1 and 2). Above ~36°

latitudes both in February and August the signs of both $\Delta\Omega_{arag\text{-}tem\text{-}spa}$ and $\Delta\Omega_{arag\text{-}nontem\text{-}spa}$ are negative; between ~36°S and ~36°N the signs of both them are positive. The same signs between $\Delta\Omega_{arag\text{-}tem\text{-}spa}$ and $\Delta\Omega_{arag\text{-}nontem\text{-}spa}$ are also caused by their intrinsic definitions. As analyzed in Section 2, by definition Ω_{arag} thermal components increase with temperature and always have a positive correlation with temperature, while similar to pH, the nonthermal components of Ω_{arag} mainly reflect the relative change between TA and DIC and present a positive correlation with [TA-DIC] (Xue & Cai, 2020). This is verified by the spatial variability of surface Ω_{arag}. $\Delta\Omega_{arag\text{-}tem\text{-}spa}$ is positively correlated with ΔSST_{spa} (Figures S2e and S3e) and always presents similar patterns to ΔSST_{spa} (Figures 1–3), whereas $\Delta\Omega_{arag\text{-}nontem\text{-}spa}$ is positively correlated with $\Delta[TA\text{-}DIC]_{spa}$ (Figures S2f and S3f) and exhibits similar patterns to $\Delta[TA\text{-}DIC]_{spa}$ (Figures 1–3). Also, we find both $\Delta[TA\text{-}DIC]_{spa}$ and $\Delta\Omega_{arag\text{-}nontem\text{-}spa}$ are positively correlated with ΔSST_{spa} (Figures 1–3 and S2, S3), which well explains the consistency between $\Delta\Omega_{arag\text{-}tem\text{-}spa}$ and $\Delta\Omega_{arag\text{-}nontem\text{-}spa}$ in signs and the similarity between $\Delta\Omega_{arag\text{-}spa}$ and ΔSST_{spa} (Figures 1–3).

Furthermore, it is worth noting that $\Delta\Omega_{arag\text{-}spa}$ is almost completely controlled by nonthermal components and the ratio between nonthermal and thermal components ($r\Omega_{arag\text{-}spa}$) is far larger than 1 (Figures 4b and 4d). During February $\Delta\Omega_{arag\text{-}tem\text{-}spa}$ ranges from −0.15 to 0.27, whereas $\Delta\Omega_{arag\text{-}nontem\text{-}spa}$ varies between −1.44 and 1.37 in the global surface ocean (Figures 1d and 1f). During August $\Delta\Omega_{arag\text{-}tem\text{-}spa}$ ranges from −0.17 to 0.25, whereas $\Delta\Omega_{arag\text{-}nontem\text{-}spa}$ varies between −1.61 and 1.31 (Figures 2d and 2f). The dominance of nonthermal components over $\Delta\Omega_{arag\text{-}spa}$ is because the thermal components have a relatively minor influence on Ω_{arag}, but a relatively important influence on pH (Cai, Xu et al., 2020; Jiang et al., 2019; Xue et al., 2017; Xue & Cai, 2020). Also, because of the in-phase between $\Delta\Omega_{arag\text{-}tem\text{-}spa}$ and $\Delta\Omega_{arag\text{-}nontem\text{-}spa}$, the reinforcing each other of these two components adds the magnitude of $\Delta\Omega_{arag\text{-}spa}$, which varies from −1.76 to 1.62 (Figures 1 and 2).

Overall, our proposed hypothesis in Section 2.1 can operate for the spatial viability of pH and Ω_{arag} and can well explain why pH and Ω_{arag} are often out of phase in spatial patterns. Given that in the global surface ocean $\Delta\Omega_{arag\text{-}spa}$ is almost completely controlled by $\Delta\Omega_{arag\text{-}nontem\text{-}spa}$ (Figure 4), when pH is controlled more by nonthermal components than by thermal components during cold seasons of both hemispheres in mid-and-high latitudes (Figure 4), pH and Ω_{arag} will be in phase since their nonthermal components are intrinsically in phase, both reflecting the variability of $\Delta[TA\text{-}DIC]_{spa}$ (Figures 3 and S2, S3). However, when pH is controlled more by thermal components during warm seasons of both hemispheres in mid-and-high latitudes, and in low-latitudes, pH and Ω_{ara} will be out of phase since the thermal and nonthermal components of pH are out of phase and the nonthermal components of both pH and Ω_{arag} are in phase. This also explains why there are low pH values and high Ω_{arag} values in the tropical and subtropical waters, that is, in low-latitudes pH is more strongly controlled by thermal components with $\Delta pH_{tem\text{-}spa} < 0$ and Ω_{ara} is dominated by nonthermal components with $\Delta\Omega_{arag\text{-}nontem\text{-}spa} > 0$. In addition, we find the partial cancellation between thermal and nonthermal components of pH leads to a relatively small spatial variability of pH compared to Ω_{arag}. In February and August, sea surface pH distribution is relatively homogeneous with ΔpH_{spa} ranging from −0.12 to 0.17, whereas Ω_{arag} shows substantial spatial variabilities with $\Delta\Omega_{arag\text{-}spa}$ varying from −1.76 to 1.62 (Figures 1 and 2).

3.2. Seasonal Cycles of Sea Surface pH and Ω_{arag}

For seasonal cycles, in the global surface ocean pH and Ω_{arag} are generally in phase in mid- and high-latitudes but out of phase in low-latitudes (Figures 5 and S5, S8), similar to previous observations (Kwiatkowski & Orr, 2018; Takahashi et al., 2014). In the North Pacific (Figures 5 and S1), for example at 48°N (mid-latitude) and at 60°N (high-latitude) sea surface pH and Ω_{arag} are generally in phase over seasonal cycles. In contrast, at 16°N (low-latitude) sea surface pH and Ω_{arag} are out of phase. Correspondingly, their seasonal amplitudes or ΔpH_{sea} and $\Delta\Omega_{arag\text{-}sea}$ show consistent signs in mid-and high-latitudes above 40°N latitudes but opposite signs in low-latitudes from ~40°S to ~40°N (Figures 6a and 6b). In the northern hemisphere, in mid-and high-latitudes north of ~40°N latitudes, both ΔpH_{sea} and $\Delta\Omega_{arag\text{-}sea}$ are positive; in contrast, from the equator to ~40°N, ΔpH_{sea} is negative while $\Delta\Omega_{arag\text{-}sea}$ is positive. In the southern hemisphere, both ΔpH_{sea} and $\Delta\Omega_{arag\text{-}sea}$ have similar features but opposite signs to those in the northern hemisphere.

3.2.1. Influence of Thermal and Nonthermal Components on pH Seasonal Cycles

To explore why pH and Ω_{arag} are often out of phase during seasonal cycles, based on the method described in Section 2.2.2, by separating pH and Ω_{arag} as well as their seasonal amplitude (ΔpH_{sea} and $\Delta\Omega_{arag\text{-}sea}$) into

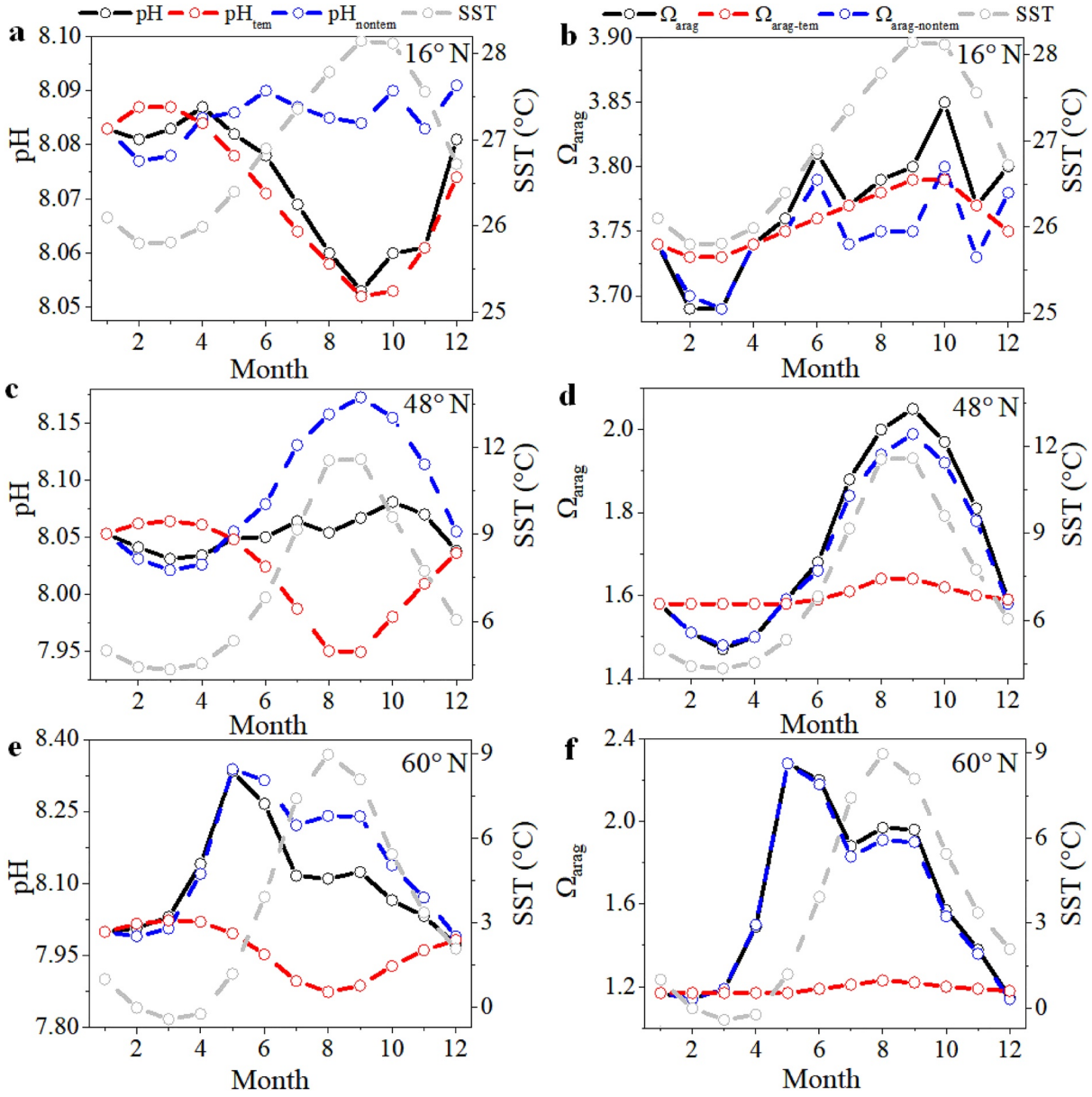

Figure 5. Seasonal cycles of climatological sea surface pH, Ω_{arag} and sea surface temperature (SST) at three grids in the North Pacific (16°N, 172.5°W; 48°N, 172.5°W; 60°N, 172.5°W). Black solid lines denote *in situ* pH or Ω_{arag}, red dashed lines denote thermal pH or Ω_{arag} just due to temperature effects (pH_{tem} or $\Omega_{arag\text{-}tem}$), blue dashed lines denote nonthermal pH or Ω_{arag} just due to non-temperature effects (pH_{nontem} or $\Omega_{arag\text{-}nontem}$), and gray dashed lines denote SST. The location of the three points is shown in Figure S1.

thermal and nonthermal components we confirm that the hypothesis proposed in Section 2.1 operates for seasonal cycles.

We find that for seasonal cycles across the global surface ocean the thermal and nonthermal components of pH are almost always out of phase, whether at low-latitudes or at mid- and high-latitudes (Figures 5 and S5, S8). Accordingly, in the global surface ocean, the thermal and nonthermal components of pH seasonal amplitude, that is, $\Delta pH_{tem\text{-}sea}$ and $\Delta pH_{nontem\text{-}sea}$ present opposite signs (Figures 6c and 6e). In the northern hemisphere, $\Delta pH_{tem\text{-}sea}$ is negative, but $\Delta pH_{nontem\text{-}sea}$ is positive; in the southern hemisphere, $\Delta pH_{tem\text{-}sea}$ is positive, but $\Delta pH_{nontem\text{-}sea}$ is negative. Similar to $\Delta pH_{tem\text{-}spa}$ and $\Delta pH_{nontem\text{-}spa}$, the opposite signs between $\Delta pH_{tem\text{-}sea}$ and $\Delta pH_{nontem\text{-}sea}$ are also caused by their intrinsic definitions as mentioned in Section 3.1.1. Therefore, $\Delta pH_{tem\text{-}sea}$ is negatively correlated with the SST seasonal amplitude or ΔSST_{sea} (Figure S4a) and

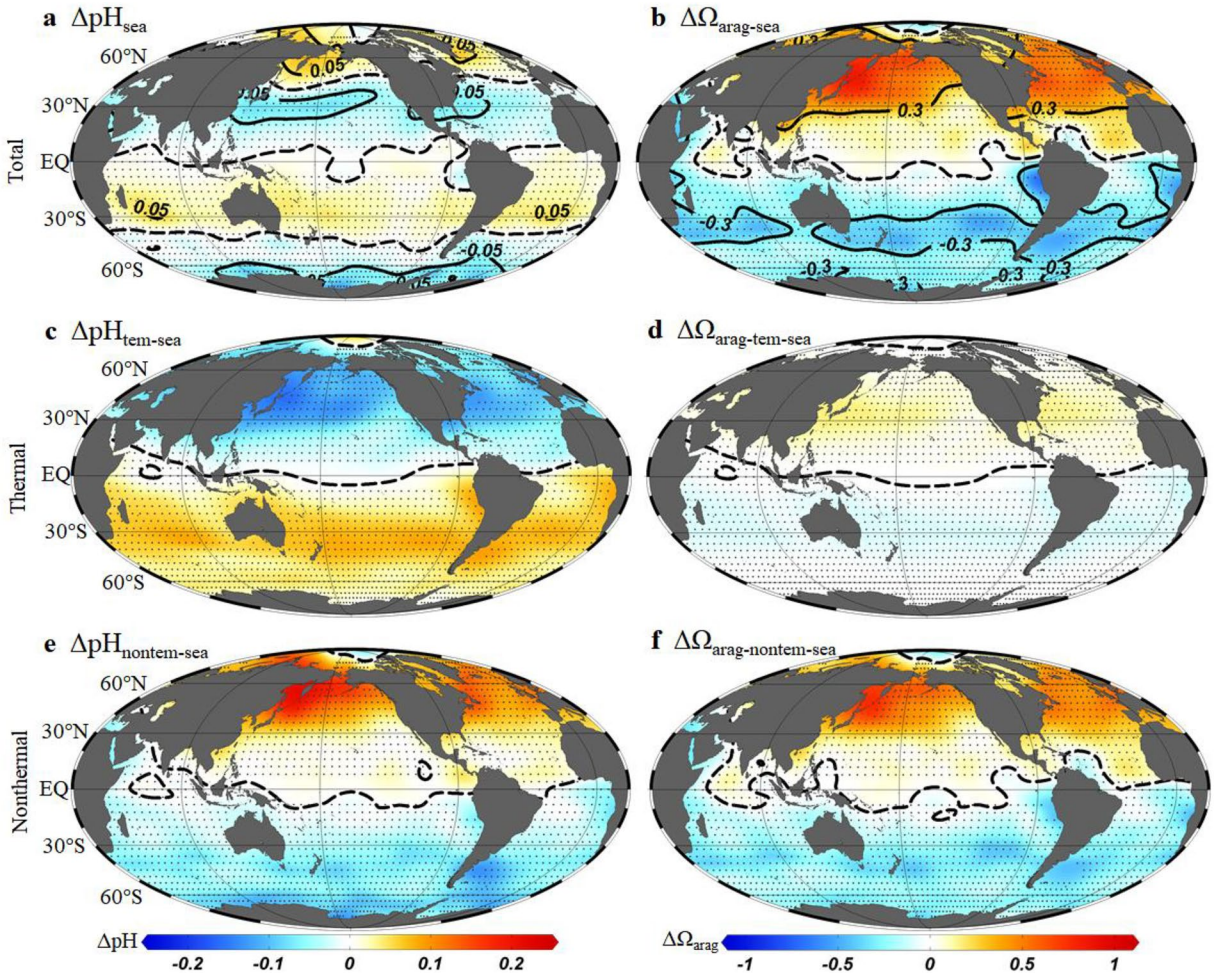

Figure 6. Seasonal amplitude of climatological sea surface pH and Ω_{arag} (ΔpH_{sea} and $\Delta\Omega_{ara-sea}$, a–b) as well as their thermal ($\Delta pH_{tem-sea}$ and $\Delta\Omega_{arag-tem-sea}$, c–d) and nonthermal components ($\Delta pH_{nontem-sea}$ and $\Delta\Omega_{arag-nontem-sea}$, e–f). The seasonal amplitude is given as the July-August-September mean value minus the January-February-March mean value as shown by Takahashi et al. (2014). Note as shown by the dots, climatological pH and Ω_{arag} data are not available in the equatorial zone (4°N–4°S) of the Pacific due to large interannual variabilities associated with ENSO events. Black lines denote isolines and the dashed ones show those with values of zero.

always presents opposite patterns to ΔSST_{sea} (Figures 3e and 6c), whereas $\Delta pH_{nontem-sea}$ is positively correlated with the seasonal amplitude of [TA-DIC] or $\Delta[TA\text{-}DIC]_{sea}$ (Figure S4b) and exhibits similar patterns to $\Delta[TA\text{-}DIC]_{sea}$ (Figures 3f and 6e). Also, we find both $\Delta[TA\text{-}DIC]_{sea}$ and $\Delta pH_{nontem-sea}$ are positively correlated with ΔSST_{sea} (Figure S4). This not only directly explains the opposite signs between $\Delta pH_{tem-sea}$ and $\Delta pH_{nontem-sea}$, but also indicates that $\Delta pH_{nontem-sea}$ or $\Delta[TA\text{-}DIC]_{sea}$ is mainly controlled by SST associated processes such as air-sea exchange, vertical mixing and biological activity (e.g., Keppler et al., 2020; Wu et al., 2019) as analyzed in Section 3.1.1.

Similar to the spatial variability, the thermal and nonthermal components of pH seasonal variability are also comparable in amplitude. In the global surface ocean, $\Delta pH_{tem-sea}$ ranges from −0.23 to 0.14, whereas $\Delta pH_{nontem-sea}$ varies between −0.19 and 0.29 (Figures 6c and 6e). As a result, the pH thermal and nonthermal components partially cancel each other and decrease its seasonal magnitude, with ΔpH_{sea} ranging from −0.18 to 0.19 in the global surface ocean (Figure 6a). Also because of this, there are three zones with very small pH seasonal change as shown by zero isolines, that is, switching from positive to negative at ~40°N, from negative to positive around the equator, and from positive to negative ~40°S (Figure 6a).

The seasonal variability of pH is also sometimes controlled more by thermal components than by nonthermal components and other times controlled more by nonthermal components, depending on their net

competing effects (Figures 4–6 and S5, S8). In mid- and high-latitudes above 40°N latitudes where the contribution from $\Delta pH_{tem\text{-}sea}$ is smaller than that from $\Delta pH_{nontem\text{-}sea}$ that is, the ratio between nonthermal components and thermal components (rpH_{sea}) > 1 (Figure 4e), ΔpH_{sea} there is controlled more by $\Delta pH_{nontem\text{-}sea}$ mainly due to the strong influence of biology and/or mixing (Takahashi et al., 2002). For example, in the North Pacific at 60°N, 172.5°W (high-latitude), when ΔSST_{sea} is 6.56°C, $\Delta pH_{tem\text{-}sea}$ is −0.13 and $\Delta pH_{nontem\text{-}sea}$ is 0.23, there is a net pH seasonal change of 0.10, indicating a stronger control of nonthermal components than thermal components. In low-latitudes from ~40°S to ~40°N where the contribution from $\Delta pH_{tem\text{-}sea}$ is generally larger than that from $\Delta pH_{nontem\text{-}sea}$ that is, rpH_{sea} < 1 (Figure 4e), ΔpH_{sea} is more controlled by thermal components ($\Delta pH_{tem\text{-}sea}$) mainly because of the temperature effect exceeding the biological effect (Takahashi et al., 2002). For example, in the North Pacific at 16°N, 172.5°W (low-latitude), when ΔSST_{sea} is 1.86°C, $\Delta pH_{tem\text{-}sea}$ is −0.03 and $\Delta pH_{nontem\text{-}sea}$ is 0.01, there is a net pH seasonal change of −0.02, indicating the dominance of thermal components. Exceptions occur in the Arabian Sea and in the equatorial areas of the Pacific and the Atlantic where the contribution from $\Delta pH_{tem\text{-}sea}$ is smaller than that from $\Delta pH_{nontem\text{-}sea}$ that is, rpH_{sea} >1 (Figure 4e) and ΔpH_{sea} is more controlled by nonthermal components mainly due to upwelling induced strong biological activities and CO_2 degassing.

The seasonal variability of pH in surface ocean is similar to that of pCO_2 which also depends on the competing effects between its thermal and nonthermal components (Gruber, Landschutzer et al., 2019; Takahashi et al., 2002). That is, the seasonal amplitude of pCO_2 is generally dominated by nonthermal components such as biology in high-latitude oceans but dominated by thermal components in low-latitude oceans (Takahashi et al., 2002). Note that the strong control of thermal components over seasonal changes of surface pH or pCO_2 in low-latitudes is associated with the timescales of air-sea CO_2 equilibrium and thermal components. In real ocean, it is almost impossible for CO_2 to reach rapid air-sea equilibrium on seasonal timescales since the air-sea CO_2 exchange rate is slow, requiring a long time of approximately one year to reach air-sea equilibrium (Sarmiento & Gruber, 2006) especially in low-latitudes because of lower wind speeds compared with in mid-and high-latitudes (Takahashi et al., 2009). In contrast, the thermal components controlled by the acid-base equilibrium of seawater CO_2 systems are almost simultaneous. Therefore, in low-latitudes (except in upwelling areas) where biology and/or mixing effects are seasonally minor, the contribution from air-sea CO_2 exchange is small and pH change is primarily controlled by thermal components. However, in mid- and high-latitudes, besides relatively rapid air-sea CO_2 exchange due to strong winds (Takahashi et al., 2009), other nonthermal components such as biology and mixing would contribute a lot to pH seasonal change (e.g., Gregor et al., 2018), resulting in the primary control of nonthermal components there (Gruber, Landschutzer et al., 2019).

3.2.2. Influence of Thermal and Nonthermal Components on Ω_{arag} Seasonal Cycles

In contrast to pH, we find for seasonal cycles across the global surface ocean the thermal and nonthermal components of Ω_{arag} are generally in phase (Figures 5 and S5, S8), an identical conclusion we derived earlier for the spatial variations. Therefore, in the global surface ocean, the thermal and nonthermal components of Ω_{arag} seasonal amplitude, that is, $\Delta\Omega_{arag\text{-}tem\text{-}sea}$ and $\Delta\Omega_{arag\text{-}nontem\text{-}sea}$ present the same sign (Figures 6d and 6f). In the northern hemisphere both $\Delta\Omega_{arag\text{-}tem\text{-}sea}$ and $\Delta\Omega_{arag\text{-}nontem\text{-}sea}$ have positive signs, and in the southern hemisphere both $\Delta\Omega_{arag\text{-}tem\text{-}sea}$ and $\Delta\Omega_{arag\text{-}nontem\text{-}sea}$ have negative signs. Similar to $\Delta\Omega_{arag\text{-}tem\text{-}spa}$ and $\Delta\Omega_{arag\text{-}nontem\text{-}spa}$, the same signs between $\Delta\Omega_{arag\text{-}tem\text{-}sea}$ and $\Delta\Omega_{arag\text{-}nontem\text{-}sea}$ are also caused by their intrinsic definitions as mentioned in Section 3.1.2. Therefore, $\Delta\Omega_{arag\text{-}tem\text{-}sea}$ is positively correlated with ΔSST_{sea} (Figure S4e) and always presents similar patterns to ΔSST_{sea} (Figures 3e and 6d), whereas similar to $\Delta pH_{nontem\text{-}sea}$, $\Delta\Omega_{arag\text{-}nontem\text{-}sea}$ is positively correlated with $\Delta[TA\text{-}DIC]_{sea}$ (Figure S4f) and exhibits similar patterns to $\Delta[TA\text{-}DIC]_{sea}$ (Figures 3e and 6f). Also, we find both $\Delta[TA\text{-}DIC]_{sea}$ and $\Delta\Omega_{arag\text{-}tem\text{-}sea}$ are positively correlated with ΔSST_{sea} (Figure S4), which well explains the consistency between $\Delta\Omega_{arag\text{-}tem\text{-}sea}$ and $\Delta\Omega_{arag\text{-}nontem\text{-}sea}$ in signs and the similarity between $\Delta\Omega_{arag\text{-}sea}$ and ΔSST_{sea} (Figures 3, 5 and 6).

Similar to the Ω_{arag} spatial variability, during seasonal cycles the contribution from the thermal component is minor relative to its nonthermal component, and the ratio between nonthermal and thermal components ($r\Omega_{arag\text{-}sea}$) is generally much larger than 1 (Figure 4f), that is, $\Delta\Omega_{arag\text{-}sea}$ is almost completely dominated by $\Delta\Omega_{arag\text{-}nontem\text{-}sea}$. For instance, in the global surface ocean $\Delta\Omega_{arag\text{-}tem\text{-}sea}$ ranges from −0.12 to 0.20, whereas $\Delta\Omega_{arag\text{-}nontem\text{-}sea}$ varies between −0.78 and 1.00 (Figures 6d and 6f). Despite this, there are exceptions in some patched areas of tropical oceans with $r\Omega_{arag\text{-}sea}$ < 1 (Figure 4f), and the reason for this remains to be further

studied. Also, the reinforcing each other of $\Delta\Omega_{arag}$ thermal and nonthermal components adds the seasonal magnitude of Ω_{arag} with $\Delta\Omega_{arag\text{-}sea}$ varying from −0.90 to 1.09 (Figures 5, 6 and S5, S8). And Ω_{arag} has only one zone with little seasonal changes as shown by zero isolines, that is, switching from negative to positive around the equator (Figure 6b).

Overall, our proposed hypothesis also can operate for seasonal cycles of pH and Ω_{arag} and can well explain why pH and Ω_{arag} are often out of phase. Given that in the global ocean Ω_{arag} is almost completely dominated by $\Delta\Omega_{arag\text{-}nontem\text{-}sea}$ (Figures 4–6 and S5, S8), when pH is controlled more by nonthermal components than by thermal components in mid- and high-latitudes, the seasonal cycles of pH and Ω_{arag} will be in phase there since their nonthermal components are intrinsically in phase, both reflecting the seasonal variability of [TA-DIC] (Figures 3, 6 and S4). Our explanation for seasonal cycles of pH and Ω_{arag} in mid- and high-latitude ocean is consistent with that by Takahashi et al. (2014) who think in the Drake Passage the in-phase between pH and Ω_{arag} is due to the dominant role by biology, that is, nonthermal effects. In contrast, when pH is dominated by thermal components in low-latitudes, pH and Ω_{arag} will be out of phase there since the thermal and nonthermal components of pH are out of phase, and the nonthermal components of both pH and Ω_{arag} are in phase. However, our explanation is different from that by Takahashi et al. (2014) in subtropical ocean. While we contend that this is because pH is more controlled by the thermal component there while Ω_{arag} is dominated by the nonthermal component, they suggest that the out-of-phase between pH and Ω_{arag} is mainly due to the different temperature effects on pH and Ω_{arag} via changing the apparent dissociation constants of carbonic acid as well as the apparent solubility product of $CaCO_3$, since increasing temperature would decrease pH but increase Ω_{arag}, that is, the different effects of thermal components on pH and Ω_{arag}. Though this explanation appears reasonable due to the in-phase between thermal and nonthermal components of Ω_{arag}, they ignore the fact that $\Omega_{arag\text{-}sea}$ is almost completely dominated by nonthermal components even in subtropical ocean (Figure 4f). Therefore, the different effects of thermal components on pH and Ω_{arag} cannot really explain the observed pH and Ω_{arag} out-of-phase behavior in low-latitude ocean. In addition, the cancellation effect between thermal and nonthermal components of pH leads to very small pH seasonal changes, appearing in three zones (Figure 6a), whereas Ω_{arag} changes from a very high positive seasonal cycle in the north to a high negative seasonal cycle in the south and has only one zone with little seasonal changes as shown by zero isolines (Figure 6b) since the thermal and nonthermal components of Ω_{arag} are generally in phase.

4. Concluding Remarks

By separating spatial and seasonal variations of both pH and Ω_{arag} into thermal and nonthermal components, we confirm our proposed hypothesis. That is, because temperature effects or thermal components present different influences on pH and Ω, pH is sometimes more controlled by nonthermal components and other times more controlled by thermal components since these two components are out of phase and comparable in magnitude. While Ω is almost always dominated by nonthermal components since thermal components have a relatively minor influence on it. This hypothesis well explains why pH and Ω_{arag} are often out of phase in spatial patterns and seasonal cycles. In mid -and high-latitudes, pH and Ω_{arag} are generally in phase in spatial patterns (cold seasons) and seasonal cycles because here pH is controlled more by nonthermal components than by thermal components and the nonthermal components of pH and Ω_{arag} are intrinsically in phase (Figure 7a), both reflecting the variability of [TA-DIC]. In contrast, in low-latitudes pH and Ω_{arag} are out of phase in spatial patterns and seasonal cycles since here pH is controlled more by thermal components (Figure 7b). Also, during warm seasons in mid-and high-latitudes, because here pH is controlled more by thermal components, pH and Ω_{arag} are out of phase in spatial patterns (Figure 7b). In addition, we show that the comparable but opposite effects of the thermal and nonthermal components on pH to a large extent decrease its magnitude both in spatial and seasonal variabilities.

This work indicates that the out-of-phase between pH and Ω_{arag} in spatial patterns and seasonal cycles originates from their contrasting thermal components. This also may be the source causing the ongoing debate as to whether pH or Ω_{arag} is a better indicator of the influences of carbonate chemistry on marine organisms (Jokiel, 2013; Riebesell, 2004; Waldbusser et al., 2014). Therefore, we infer that both pH and Ω_{arag} would be good indicators of the influences of carbonate chemistry on marine organisms, if experiments about OA influences on organisms are conducted at constant temperatures, which removes influences from thermal

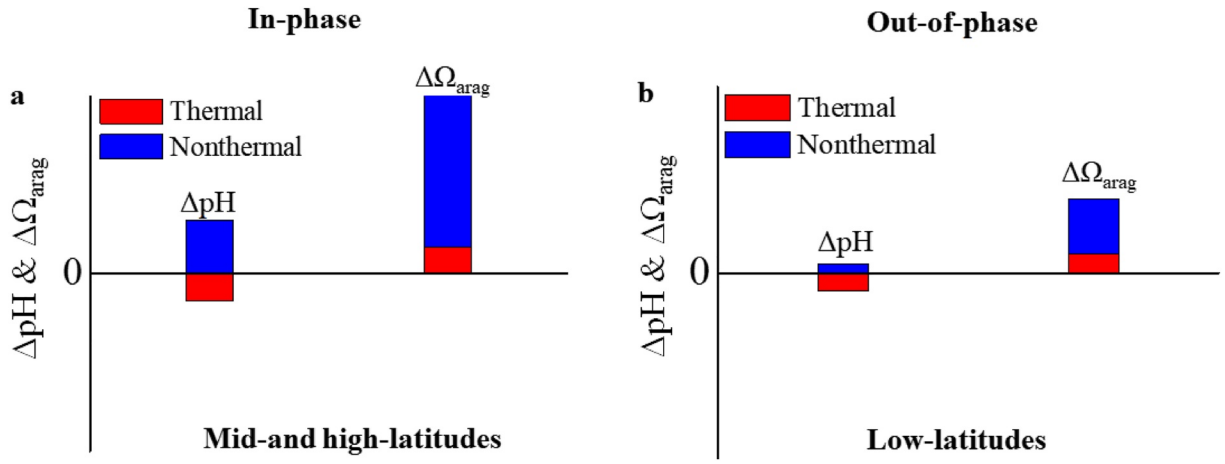

Figure 7. A schematic illustration showing why pH and Ω_{arag} sometimes are in phase and other times are out of phase. In this figure, red color denotes thermal components, while blue color nonthermal components. A total change of pH or Ω_{arag} depends on the net balance of thermal and nonthermal components. When pH is dominated by nonthermal components such as in mid- and high-latitudes, pH and Ω_{arag} will be in phase in spatial patterns and seasonal cycles (a); when pH is dominated by thermal components for example in low-latitudes, pH and Ω_{arag} will be out of phase (b). Note that for surface spatial patterns in mid- and high-latitudes during cold seasons pH is generally controlled by nonthermal components, while during warm seasons pH is controlled by thermal components (see Figure 4).

components. In addition, across the global surface ocean pH in the tropical waters and Ω_{arag} in the polar waters are lower than the respective global mean value (Figures 1 and 2). Thus, from this point of view, one may choose pH in the tropical waters and Ω_{arag} in the polar waters as a bellwether or a better indicator for OA. Overall, this work would help better understand the similarities and differences between the two commonly used OA parameters as well as their biological influences.

Conflict of Interest

The authors declare no conflicts of interest relevant to this study.

Data Availability Statement

Data used in this study are from the LDEO Takahashi Database (https://www.nodc.noaa.gov/ocads/oceans/ndp_094/ndp094.html or doi: 10.3334/cdiac/otg.ndp094).

Acknowledgments
This work was supported by the Basic Scientific Fund for National Public Research Institutes of China [2019S05], the Global Change and Air-sea Interaction Project [GASI-04-QYQH-02], the Marine S&T Fund of Shandong Province for Pilot National Laboratory for Marine Science and Technology (Qingdao) [No.2018SDKJ0105-3], China Ocean Mineral Resources R & D Association [DY135-E2-4-03] and the Monsoon Onset Monitoring and its Social and Ecosystem Impact (MOMSEI) program. Funding for L-QJ was from NOAA Ocean Acidification Program (OAP, Project ID: 1842–1210).

References

Cai, W.-J., Feely, R. A., Testa, J. M., Li, M., Evans, W., Alin, S. R., et al. (2020). Natural and anthropogenic drivers of acidification in large estuaries. *Annual Review of Marine Science*, *13*(1). https://doi.org/10.1146/annurev-marine-010419-011004

Cai, W.-J., Xu, Y., Feely, R. A., Wanninkhof, R., Jönsson, B., Alin, S. R., et al. (2020). Controls on surface water carbonate chemistry along North American ocean margins. *Nature Communications*, *11*, 2691. https://doi.org/10.1038/s41467-020-16530-z

Caldeira, K., & Wickett, M. E. (2003). Oceanography: Anthropogenic carbon and ocean pH. *Nature*, *425*(6956), 365. https://doi.org/10.1038/425365a

Cooley, S. R., Mathis, J. T., Yates, K. K., & Turley, C. (2012). Frequently asked questions about ocean acidification. U.S. Ocean Carbon and Biogeochemistry Program and the UK Ocean Acidification Research Programme, Version 2. 24 September 2012. Retrieved from www.whoi.edu/OCB-OA/FAQs

Dickson, A. G., & Millero, F. J. (1987). A comparison of the equilibrium constants for the dissociation of carbonic acid in seawater media. *Deep Sea Research Part A, Oceanographic Research Papers*, *34*(10), 1733–1743. https://doi.org/10.1016/0198-0149(87)90021-5

Doney, S. C., Busch, D. S., Cooley, S. R., & Kroeker, K. J. (2020). The impacts of ocean acidification on marine ecosystems and reliant human communities. *Annual Review of Environment and Resources*, *45*(1), 83–112. https://doi.org/10.1146/annurev-environ-012320-083019

Doney, S. C., Fabry, V. J., Feely, R. A., & Kleypas, J. A. (2009). Ocean acidification: The other CO_2 problem. *Annual Review of Marine Science*, *1*(1), 169–192. https://doi.org/10.1146/annurev.marine.010908.163834

Dore, J. E., Lukas, R., Sadler, D. W., Church, M. J., & Karl, D. M. (2009). Physical and biogeochemical modulation of ocean acidification in the central North Pacific. *Proceedings of the National Academy of Sciences*, *106*(30), 12235–12240. https://doi.org/10.1073/pnas.0906044106

Fabry, V. J., McClintock, J. B., Mathis, J. T., & Grebmeier, J. M. (2009). Ocean acidification at high latitudes: The bellweather. *Oceanography*, *22*(4), 160–171. https://doi.org/10.5670/oceanog.2009.105

Gieskes, J. M. (1969). Effect of temperature on the pH of seawater. *Limnology & Oceanography*, *14*(5), 679–685. https://doi.org/10.4319/lo.1969.14.5.0679

Gregor, L., Kok, S., & Monteiro, P. M. S. (2018). Interannual drivers of the seasonal cycle of CO_2 in the Southern Ocean. *Biogeosciences*, *15*(8), 2361–2378. https://doi.org/10.5194/bg-15-2361-2018

Gruber, N., Clement, D., Carter, B. R., Feely, R. A., Steven, V. H., Hoppema, M., et al. (2019). The oceanic sink for anthropogenic CO_2 from 1994 to 2007. *Sciences*, *363*(6432), 1193–1199. https://doi.org/10.1126/science.aau5153

Gruber, N., Landschützer, P., & Lovenduski, N. S. (2019). The variable Southern Ocean carbon sink. *Annual Review of Marine Science*, *11*(1), 159–186. https://doi.org/10.1146/annurev-marine-121916-063407

Jiang, L.-Q., Carter, B. R., Feely, R. A., Lauvset, S. K., & Olsen, A. (2019). Surface ocean pH and buffer capacity: Past, present and future. *Scientific Reports*, *9*. https://doi.org/10.1038/s41598-019-55039-4

Jiang, L.-Q., Feely, R. A., Carter, B. R., Greeley, D. J., Gledhill, D. K., & Arzayus, K. M. (2015). Climatological distribution of aragonite saturation state in the global oceans. *Global Biogeochemical Cycles*, *29*, 1656–1673. https://doi.org/10.1002/2015GB005198

Jokiel, P. L. (2013). Coral reef calcification: Carbonate, bicarbonate and proton flux under conditions of increasing ocean acidification. *Proceedings of the Royal Society B: Biological Sciences*, *280*(1764), 529–549. https://doi.org/10.1098/rspb.2013.0031

Keppler, L., Landschützer, P., Gruber, N., Lauvset, S. K., & Stemmler, I. (2020). Seasonal carbon dynamics in the near-global ocean. *Global Biogeochemical Cycles*, *34*, e2020GB006571. https://doi.org/10.1029/2020GB006571

Kwiatkowski, L., & Orr, J. C. (2018). Diverging seasonal extremes for ocean acidification during the twenty-first century. *Nature Climate Change*, *8*(2), 141–145. https://doi.org/10.1038/s41558-017-0054-0

Landschützer, P., Gruber, N., Bakker, D. C. E., Stemmler, I., & Six, K. D. (2018). Strengthening seasonal marine CO_2 variations due to increasing atmospheric CO_2. *Nature Climate Change*, *8*(2), 146–150. https://doi.org/10.1038/s41558-017-0057-x

Lauvset, S. K., Gruber, N., Landschützer, P., Olsen, A., & Tjiputra, J. (2015). Trends and drivers in global surface ocean pH over the past 3 decades. *Biogeosciences*, *12*(5), 1285–1298. https://doi.org/10.5194/bg-12-1285-2015

Lewis, E., & Wallace, D. W. R. (1998). *Program developed for CO_2 systems calculations*.

McNeil, B. I., & Matear, R. J. (2008). Southern Ocean acidification: A tipping point at 450-ppm atmospheric CO_2. *Proceedings of the National Academy of Sciences*, *105*(48), 18860–18864. https://doi.org/10.1073/pnas.0806318105

Mcneil, B. I., & Sasse, T. P. (2016). Future ocean hypercapnia driven by anthropogenic amplification of the natural CO_2 cycle. *Nature*, *529*(7586), 383–387. https://doi.org/10.1038/nature16156

Mehrbach, C., Culberson, C. H., Hawley, J. E., & Pytkowicz, R. M. (1973). Measurement of the apparent dissociation constants of carbonic acid in seawater at atmospheric pressure. *Limnology & Oceanography*, *18*(6), 897–907. https://doi.org/10.4319/lo.1973.18.6.0897

Morse, J. W., Arvidson, R. S., & Lüttge, A. (2007). Calcium carbonate formation and dissolution. *Chemical Reviews*, *107*(2), 342–381. https://doi.org/10.1021/cr050358j

Mucci, A. (1983). The solubility of calcite and aragonite in seawater at various salinities, temperatures, and one atmosphere total pressure. *American Journal of Science*, *283*(7), 780–799. https://doi.org/10.2475/ajs.283.7.780

Riebesell, U. (2004). Effects of CO_2 enrichment on marine phytoplankton. *Journal of Oceanography*, *60*(4), 719–729. https://doi.org/10.1007/s10872-004-5764-z

Riley, J. P., & Tongudai, M. (1967). The major cation/chlorinity ratios in sea water. *Chemical Geology*, *2*, 263–269. https://doi.org/10.1016/0009-2541(67)90026-5

Sarmiento, J. L., & Gruber, N. (2006). *Ocean biogeochemical dynamics*. Princeton University Press.

Schlitzer, R. (2018). *Ocean Data view*. Retrieved from http://odv.awi.de

Takahashi, T., Sutherland, S. C., Chipman, D. W., Goddard, J. G., & Ho, C. (2014). Climatological distributions of pH, pCO_2, total CO_2, alkalinity, and $CaCO_3$ saturation in the global surface ocean, and temporal changes at selected locations. *Marine Chemistry*, *164*, 95–125. https://doi.org/10.1016/j.marchem.2014.06.004

Takahashi, T., Sutherland, S. C., Sweeney, C., Poisson, A., Metzl, N., Tilbrook, B., et al. (2002). Global sea-air CO_2 flux based on climatological surface ocean pCO_2, and seasonal biological and temperature effects. *Deep-Sea Research Part II*, *49*(9–10), 1601–1622. https://doi.org/10.1016/s0967-0645(02)00003-6

Takahashi, T., Sutherland, S. C., Wanninkhof, R., Sweeney, C., Feely, R. A., Chipman, D. W., et al. (2009). Climatological mean and decadal change in surface ocean pCO_2, and net sea-air CO_2 flux over the global oceans. *Deep-Sea Research Part II*, *56*(8–10), 554–577. https://doi.org/10.1016/j.dsr.2009.07.007

van Heuven, S., Pierrot, D., Lewis, E., & Wallace, D. W. R. (2009). *MATLAB program developed for CO_2 system calculations. ORNL/CDIAC-105b, carbon dioxide information analysis center*. Oak Ridge National Laboratory, U.S. Department of Energy.

Waldbusser, G. G., Hales, B., Langdon, C. J., Haley, B. A., Schrader, P., Brunner, E. L., et al. (2014). Saturation-state sensitivity of marine bivalve larvae to ocean acidification. *Nature Climate Change*, *5*, 273–280. https://doi.org/10.1038/NCLIMATE2479

Wang, Y., Fan, X., Gao, G., Beardall, J., Inaba, K., Hall-Spencer, J. M., et al. (2020). Decreased motility of flagellated microalgae long-term acclimated to CO_2-induced acidified waters. *Nature Climate Change*, *10*(6), 561–567. https://doi.org/10.1038/s41558-020-0776-2

Weiss, R. F. (1974). Carbon dioxide in water and seawater: The solubility of a non-ideal gas. *Marine Chemistry*, *2*, 203–215. https://doi.org/10.1016/0304-4203(74)90015-2

Wu, Y., Hain, M. P., Humphreys, M. P., Hartman, S., & Tyrrell, T. (2019). What drives the latitudinal gradient in open-ocean surface dissolved inorganic carbon concentration? *Biogeosciences*, *16*(13), 2661–2681. https://doi.org/10.5194/bg-16-2661-2019

Xu, Y.-Y., Cai, W.-J., Wanninkhof, R., Salisbury, J., Reimer, J., & Chen, B. (2020). Long-term changes of carbonate chemistry variables along the North American East coast. *Journal of Geophysical Research: Oceans*, *125*, e2019JC015982. https://doi.org/10.1029/2019JC015982

Xue, L., & Cai, W.-J. (2020). Total alkalinity minus dissolved inorganic carbon as a proxy for deciphering ocean acidification mechanisms. *Marine Chemistry*, *222*. https://doi.org/10.1016/j.marchem.2020.103791

Xue, L., Cai, W.-J., Sutton, A. J., & Sabine, C. (2017). Sea surface aragonite saturation state variations and control mechanisms at the Gray's Reef time-series site off Georgia, USA (2006–2007). *Marine Chemistry*, *195*, 27–40. https://doi.org/10.1016/j.marchem.2017.05.009

Xue, L., Wang, H., Jiang, L.-Q., Cai, W.-J., Wei, Q., Song, H., et al. (2016). Aragonite saturation state in a monsoonal upwelling system off Java, Indonesia. *Journal of Marine Systems*, *153*, 10–17. https://doi.org/10.1016/j.jmarsys.2015.08.003

Xue, L., Yang, X., Li, Y., Li, L., Jiang, L.-Q., Xin, M., et al. (2020). Processes controlling sea surface pH and aragonite saturation state in a large northern temperate bay: Contrasting temperature effects. *Journal of Geophysical Research: Biogeosciences*, *125*, e2020JG005805. https://doi.org/10.1029/2020JG005805